Original Article

MOLECULAR METABOLISM

# Adipose PTEN regulates adult adipose tissue homeostasis and redistribution via a PTEN-leptin-sympathetic loop

Wei Huang [1,2,3], Nicholas J. Queen [1,2,3], Travis B. McMurphy [1,2,3], Seemaab Ali [1,2], Lei Cao [1,2,*]

## ABSTRACT

**Objective:** Despite the large body of work describing the tumor suppressor functions of Phosphatase and tensin homologue deleted on chromosome ten (PTEN), its roles in adipose homeostasis of adult animals are not yet fully understood. Here, we sought to determine the role of PTEN in whole-body adipose homeostasis.

**Methods:** We genetically manipulated PTEN in specific fat depots through recombinant adeno-associated viral vector (rAAV)-based gene transfer of Cre recombinase to adult $PTEN^{flox}$ mice. Additionally, we used a denervation agent, 6OHDA, to assess the role of sympathetic signaling in PTEN-related adipose remodeling. Furthermore, we chemically manipulated AKT signaling via a pan-AKT inhibitor, MK-2206, to assess the role of AKT in PTEN-related adipose remodeling. Finally, to understand the role of leptin and central signaling on peripheral tissues, we knocked down hypothalamic leptin receptor with a microRNA delivered by a rAAV vector.

**Results:** Knockdown PTEN in individual fat depot resulted in massive expansion of the affected fat depot through activation of AKT signaling associated with suppression of lipolysis and induction of leptin. This hypertrophic expansion of the affected fat depot led to upregulation of PTEN level, higher lipolysis, and induction of white fat browning in other fat depots, and the compensatory reduced fat mass to maintain a set point of whole-body adiposity. Administration of AKT inhibitor MK-2206 prevented the adipose PTEN knockdown-associated effects. 6OHDA-mediated denervation demonstrated that sympathetic innervation was required for the PTEN knockdown-induced adipose redistribution. Knockdown hypothalamic leptin receptor attenuated the adipose redistribution induced by PTEN deficiency in individual fat depot.

**Conclusions:** Our results demonstrate the essential role of PTEN in adipose homeostasis, including mass and distribution in adulthood, and reveal an "adipose PTEN-leptin-sympathetic nervous system" feedback loop to maintain a set point of adipose PTEN and whole-body adiposity.



**Keywords** PTEN; Leptin; Adipose; Homeostasis; Hypothalamus; Redistribution

## 1. INTRODUCTION

Adipose tissue is a dynamic endocrine organ which serves not only as a fat storage site but also to secrete adipokines to exert systemic effects [1]. Adipose tissue mass expands through hypertrophy and hyperplasia and is subjected to neuronal, hormonal, and nutritional regulations [2]. Of particular importance to physiological adipose tissue homeostasis is a neural—adipose axis. Sympathetic innervation to adipose tissue has been reported in many previous studies [3]. Recent work suggests that sympathetic fibers establish neuro-adipose junctions, directly 'enveloping' adipocytes [4]. A later study reports that sympathetic fibers show close apposition to over 90% of adipocytes in adipose tissue [5]. Such sympathetic innervation drives lipolysis when mice are fasting, exposed to cold, and placed in an enriched environment [6,7]. Adipose lipolysis by sympathetic stimulation involves G-protein-coupled receptors, including β3-adrenergic receptor in a Protein kinase A (PKA) and cyclic adenosine monophosphate (cAMP) dependent manner [8]. One key target of PKA is hormone-sensitive lipase (HSL) which, together with other esterases, facilitates hydrolysis of triglycerides in adipose tissue [8].

Phosphatase and tensin homologue deleted on chromosome ten (PTEN) is a dual protein and lipid phosphatase with well-documented tumor suppressor functions [9,10]. The lipid phosphatase actions of PTEN also make it a potent regulator of cellular growth, survival, and

[1]Department of Cancer Biology and Genetics, College of Medicine, The Ohio State University, Columbus, OH 43210, USA [2]The Ohio State University Comprehensive Cancer Center, Columbus, OH 43210, USA

[3] These authors contributed equally to this work.

*Corresponding author. 460 W 12th Ave, Columbus, OH 43210, USA. Fax: +1 614 2926356. E-mail: lei.cao@osumc.edu (L. Cao).

*Abbreviations:* Adeno-associated virus, AAV; brown adipose tissue, BAT; chicken β-actin, CBA; gonadal white adipose tissue, gWAT; hypothalamus, HYP; inguinal white adipose tissue, iWAT; leptin receptor, Lepr; microRNA targeting leptin receptor, miR-LepR; microRNA targeting a scrambled sequence which targets no known gene, miR-Scr; mesenteric white adipose tissue, mWAT; Phosphatase and tensin homologue deleted on chromosome ten, PTEN; recombinant adeno-associated virus, rAAV; retroperitoneal white adipose tissue, rWAT; woodchuck post-transcriptional regulatory element, WPRE; 6-hydroxydopamine, 6OHDA

Received August 26, 2019 • Revision received September 20, 2019 • Accepted September 22, 2019 • Available online 28 September 2019

https://doi.org/10.1016/j.molmet.2019.09.008

 

insulin mediated glucose uptake [11–13]. Transgenic mouse studies implicate the role of PTEN in adipose tissue development although different models reveal inconsistent phenotypes. The aP2-Cre mediated adipose-specific PTEN knockout ($PTEN^{-/-}$) mouse line exhibits improved systematic insulin sensitivity and is resistant to streptozotocin-induced diabetes, whereas loss of PTEN in adipose tissue does not alter any fat depot adiposity [14]. In contrast, one recent study reports that inducible PTEN knockout in adipose tissue of adult mice increases adipose tissue mass via hyperplasia associated with enhanced insulin sensitivity [15]. Another study demonstrates that PTEN loss specific in the $Myf5^{+}$ adipocyte lineages leads to selective expansion of $Myf5^{+}$ adipocyte lineages, while restricting other adipocyte lineages. As a result, differences in $PI_3K$ activity between adipocytes lineages alter body fat redistribution [16]. On the other hand, the transgenic mice globally overexpressing PTEN ($PTEN^{tg}$) show reduced body size, fat accumulation and increased energy expenditure, a hyper-activation of brown fat function, elevated energy expenditure, and leanness [17,18]. Others report that adipocyte enhancer binding protein1 (AEBP1) and fatty acid binding protein modulates adipogenesis by interacting with PTEN [19,20]. Although depleting or overexpressing PTEN—during adipogenesis or in the germline—demonstrates the influence of PTEN on adipocyte differentiation, these studies provide few insights into the role of PTEN in the mature adipose remodeling process. Because fat depots are variable in their distribution and origin, studies based on *in vivo* PTEN knockout in every adipocyte of mature adipose tissue may not be well-equipped to address heterogeneity of adipose tissue in response to environmental cues and cross-talk among fat depots.

Recently, we developed a novel engineered hybrid serotype adeno-associated virus (AAV), Rec2 (AAV-Rec2). This hybrid serotype achieves superior transduction of adipose tissue when compared to the naturally occurring AAV serotypes and allows for genetic manipulation of fat depots of interest *in vivo* [21–23]. Others have applied the Rec2 serotype vectors to manipulate adipose tissues in various mouse models [24–26]. To improve selectivity of adipose transduction, we generated a novel AAV expression plasmid harboring two expression cassettes—one using the non-selective CBA promoter to drive transgene expression, and the other using a liver-specific albumin promoter to drive a microRNA targeting the woodchuck post-transcriptional regulatory element (WPRE) sequence that only exists in this rAAV vector. The dual cassette vector achieves highly selective transduction of visceral fats while severely restricting off-target transduction of liver by intraperitoneal administration [22,27]. Here, we use this unique delivery system to manipulate PTEN expression in an individual fat depot to investigate how PTEN modulates fat depots distribution in adult mouse and discover a PTEN-leptin-sympathetic signaling loop that regulates adipose redistribution.

## 2. MATERIAL AND METHODS

**Mice**. $PTEN^{flox}$ C57Bl/6 breeders were purchased from Jackson Lab (Stock No: 006440) to establish a colony. Sex and age of mice were indicated in each experiment. All use of animals was approved by, and in accordance with the Ohio State University Animal Care and Use Committee. Mice were housed in temperature (22–23 °C) and humidity-controlled rooms with food and water *ad libitum*. We fed the mice with normal chow diet (NCD, 11% fat, caloric density 3.4 kcal/g, Teklad).

**rAAV vector construction and packaging**. The rAAV plasmid contains a vector expression cassette consisting of the CMV enhancer and chicken β-actin (CBA) promoter, woodchuck post-transcriptional regulatory element (WPRE) and bovine growth hormone poly-A flanked by AAV2 inverted terminal repeats. rAAV serotype Rec2 vectors for PTEN and Cre recombinase included a second cassette encoding a microRNA driven by the albumin promoter to prevent transgene expression in the liver. The sequence of dual cassette design with Cre transgene is shown in Supplementary sequence file. Vectors were constructed as previously described [22]. The details of generation of Rec2 serotype are described before [28].

**Unilateral Injections of Rec2-Cre to the iWAT.** Male $PTEN^{flox}$ mice, 9 weeks of age, received unilateral injections to the iWAT of Rec2-Cre. The contralateral iWAT deposit was manipulated identically, but Rec2-Empty was administered instead. Surgical injections of rAAV vectors to the iWAT were performed as previously described [21,29]. Briefly, animals were anesthetized with 2% isoflurane. Surgical sites were shaved and sanitized with Betadine and 70% ethanol. A roughly 1.5 cm incision in the skin was made to expose the iWAT. A single injection was administered into the center of the adipose depot, containing a dose of $2 \times 10^{10}$ viral genomes, diluted in 20 μL AAV buffer. Surgical wounds were closed with 4-0 PDS II FS-2 sutures. Administration of Rec2-Cre was alternated between anatomical right and left iWAT depots.

**Intraperitoneal Injections of Rec2-Cre.** Female $PTEN^{flox}$ C57Bl/6 mice, 9 weeks of age, were randomly assigned to receive a single intraperitoneal injection of Rec2-Cre or Rec2-Empty as previously described [22] at the dose of $2.0 \times 10^{10}$ viral genomes diluted in AAV buffer to a volume of 100 μL.

**AKT inhibitor study.** A mixture of MK-2206 (MedChem Express #HY-10358) was created at a concentration of 3.5 mg/mL in saline. MK-2206 has low solubility in water and saline, so the mixture was warmed in a water bath at 37 °C for 10 min. The mixture was then sonicated in a water bath (VWR model 50T) for 15 s and vortexed multiple times. When the solution appeared homogenous, aliquots were made and stored at −20 °C for later use. Age-matched male $PTEN^{flox}$ mice were randomly assigned to receive Rec2- Cre ($n = 10$) or AAV viral dilution buffer ($n = 7$) via IP injection at a dose of $1.5 \times 10^{10}$ vg/100 μL/mouse. Two weeks following viral injection, IP MK-2206 administration began at a dose of 50 mg/kg every two days for 9 total doses. Serum and adipose tissues were collected for analysis at the end of study.

**rAAV-microRNA vector construction.** MicroRNAs were created to target mouse full length leptin receptor (miR-Lepr). Two targeting sequences were selected according to Invitrogen's RNAi Designer (www.invitrogen.com/rnai) and firstly cloned into the Block-iT Pol II miR RNAi Expression vector (pcDNA6.2-Gw/miR, Invitrogen) and then cut and ligated into our rAAV plasmid with a CBA promoter [30]. To select the most effective microRNA, the miR-Lepr expressing plasmids were co-transfected with a LepR expression plasmid (Lepr, MR226855, ORIGENE) to HEK293T cells. Western blotting showed the miR-Lepr with targeting sequence of 5′-TATCGTTGCTGACCAGAGTTG-3′ knocked down the Lepr expression approximately 50% in culture (data not shown). This miR-Lepr was selected for *in vivo* study. A scrambled miRNA (miR-Scr, a scrambled sequence targeting no known gene, Invitrogen) was used as a control and was cloned into the rAAV backbone plasmid. rAAV serotype 1 vectors carrying miR-Lepr or miR-Scr were packaged and purified as described previously [30].

**Hypothalamic leptin receptor knockdown experiment**. Age-matched male $PTEN^{flox}$ mice were randomly assigned to two groups and injected with AAV1-miR-Lepr or AAV1-miR-Scr ($1.0 \times 10^{10}$ particles/1.0 μL per side) bilaterally into the arcuate/ventromedial hypothalamus (AP: -1.20 mm, ML: ±0.50 mm, DV: -6.20). Stereotaxic surgery was performed as previously described [31]. Two weeks after

 

stereotaxic surgery, each miR-injected group was randomized to receive adipose injections of Rec2-Cre or Rec2-Empty to the anatomical right iWAT depot. Five weeks after Rec2-Cre injection, the four groups of mice: miR-Scr/Empty, miR-Scr/Cre, miR-Lepr/Empty, and miR-Lepr/Cre were euthanized. Serum, hypothalamic tissue, and adipose tissues were obtained for further analysis.

**Sympathetic denervation of the iWAT in PTEN knockdown study.** Male PTEN$^{flox}$ C57BL/6 mice, 9 weeks of age, were randomly assigned to receive a single intraperitoneal injection of Rec2-Cre or Rec2-Empty. Three days after viral injection, we performed a chemical denervation. Unilateral denervation of the iWAT was achieved through surgical exposure of the inguinal adipose depot followed by low volume injections of 6OHDA. One side of the inguinal adipose received five injections evenly distributed throughout the tissue, with 6 μL of 8 mg/mL 6OHDA in 0.01 M PBS plus 1% ascorbic acid. The contralateral depot was handled identically but injected with vehicle (0.01 M PBS plus 1% ascorbic acid).

**Serum harvest and biomarkers measurement**. Trunk blood was collected at euthanasia. We prepared serum by allowing the blood to clot for 30 min on ice followed by centrifugation. Serum was diluted at least 1:10 in serum assay diluent and assayed using the following ELISA kits: mouse Adiponectin (R&D Systems #DY119) and Leptin (R&D Systems #DY498). Glucose (Cayman Chemical # 10009582) and triglycerides (Cayman Chemical # 10010303) were measured using colorimetric assay kits. Insulin was measured using an ultrasensitive mouse insulin ELISA (Alpco Diagnostic #80-INSMSU-E01).

**Hypothalamic Microdissection.** Brains were quickly isolated, and the hypothalamus was dissected from 2 mm-thick-coronal sections (−0.7 ~ -2.7 mm from bregma, 1.5 mm dorsal to the bottom of the brain, 1 mm bilateral to the midline) under a dissection scope. The hypothalamus block sections were rapidly frozen at −80 °C.

**Western Blotting.** Tissue samples were homogenized in ice-cold RIPA buffer (Pierce #89901) containing 1x Phosstop (Roche #4906845001) and protease inhibitor cocktail III (Calbiochem #539134). Tissue lysates were separated by gradient gel (4−20%, Mini-PROTEAN TGX, Bio-Rad #4561096), transferred to a nitrocellulose membrane (Bio-Rad #1620115). Blots were incubated overnight at 4 °C with the following primary antibodies, Actin (Cell Signaling #4970, 1:1000), phospho-AKT- Ser$^{473}$ (Cell Signaling #9271, 1:1000), phospho-AKT-Thr$^{308}$ (Cell Signaling #9275, 1:1000), total AKT (Cell Signaling #9272, 1:1000), PTEN (Cell Signaling #9552, 1:1000), Vinculin (Cell Signaling #46050, 1:1000), PGC1-α (Cell Signaling #2178, 1:500), UCP-1 (Abcam #ab23841, 1:1000), phosphor-HSL-Ser$^{660}$ (Cell Signaling #4126, 1:1000), and HSL (Cell Signaling #4107, 1:1000). Blots were rinsed and incubated with HRP-conjugate secondary antibody (Bio-Rad). Chemiluminescence signal was detected and visualized by LI-COR Odyssey Fc imaging system (LI-COR Biotechnology, Lincoln, NE). Quantification analysis was carried out with image studio software version 5.2 (LI-COR Biotechnology).

**Quantitative RT-PCR.** We isolated total RNA using RNeasy Lipid Kit plus RNase-free DNase treatment (Qiagen #74804). We generated first-strand cDNA using TaqMan Reverse Transcription Reagent (Applied Biosystems #N8080234) and carried out quantitative PCR using StepOnePlus Real-Time PCR System (Applied Biosystems) with the Power SYBR Green PCR Master Mix (Applied Biosystems #A25742). Primer sequences are shown in Supplementary Table. We calibrated data to endogenous control Actb or Hprt1 and quantified the relative gene expression using the $2^{-\Delta\Delta CT}$ method [32].

**H&E staining and image analysis**. A portion of fat depots were fixed in 10% formalin. Paraffin sections (4 μm) were processed and H&E staining were performed by the Comparative Pathology and Mouse Phenotyping and Histology/Immunohistochemistry (CPMPSR) core of the Ohio State University Comprehensive Cancer Center. Adipose tissue sections were imaged at 20× magnification using a Nikon Eclipse 50i microscope with an Axiocam 506 color camera attachment through ZEN 2 software. For each field, adipocyte area was measured in FIJI using a semi-automated custom method based on the Adiposoft algorithm [33−35]. Briefly, each image was split into H&E color channels by Color Deconvolution, then made binary by the Otsu thresholding algorithm [36]. The images were then filtered with opening and median operators with the Morphological Filters plugin to sharpen cell boundaries [37]. Automated particle subtraction and manual removal of extraneous particles were performed to reduce noise. In white adipose tissue, a cutoff of 100 μm$^2$ was used as the minimum size for an adipocyte.

### 2.1. Statistical analysis

Data are expressed as means ± SEM. JMP, IBM SPSS v.25, and GraphPad Prism 7 statistical software were used to analyze data. The Student's t test was utilized for comparisons between two groups. For the MK-2206 and miR-Lepr studies, two-way ANOVAs were performed with the Holm-Sidak *post hoc* test for pairwise comparisons.

### 2.2. Data availability

The datasets generated during and/or analyzed during the current study are available from the corresponding author upon request.

### 2.3. Resource availability

The dual-cassette AAV expression plasmid containing Cre transgene and AAV expression plasmid containing miR-Lepr generated during the current study are available from the corresponding author upon request.

## 3. RESULTS

### 3.1. Unilateral knockdown of PTEN in the inguinal adipose tissue

To investigate the consequences of reduced PTEN levels in the adipose tissue, we utilized a dual-cassette, adipose-targeting rAAV-Rec2 vector [22] to deliver Cre recombinase to the inguinal white adipose tissue (iWAT) in PTEN$^{flox}$ mice. Nine-week-old male PTEN$^{flox}$ mice received direct injections containing $2.0 \times 10^{10}$ viral genomic particle (vg) of Rec2-Cre to one side of iWAT. The contralateral side of iWAT depot was injected identically with $2.0 \times 10^{10}$ vg of Rec2 vector carrying the same expression cassettes but no transgene (Rec2-Empty). We have previously demonstrated that inguinal fat pad injection of rAAV-Rec2-GFP with the CBA promoter shows no transgene expression in muscle, kidney, and only scarce transgene positive cells in liver [21], indicating local injection causes a limited leak in the circulation. The use of a dual-cassette liver-restricting vector further prevented off-target transgene expression [22].

Age- and weight-matched untreated PTEN$^{flox}$ animals were included as an additional control. Animals were sacrificed 7 weeks post rAAV injection. Rec2-Cre treatment dramatically expanded the transduced iWAT depot while significantly reducing the size of the contralateral iWAT pad (Rec2-Empty injected) in comparison to PTEN$^{flox}$ controls (Figure 1A—C). Browning of the contralateral iWAT was visually apparent (Figure 1C). Total gonadal WAT (gWAT), retroperitoneal WAT (rWAT), and brown adipose tissue (BAT) were substantially reduced in Rec2-Cre treated animals (Figure 1A,B). Although the contralateral iWAT was smaller, the massive increase in Rec2-Cre treated iWAT led to an increase in total iWAT weight (Figure 1A). No significant changes were seen in body or liver weights (Figure 1A). H&E staining of

 

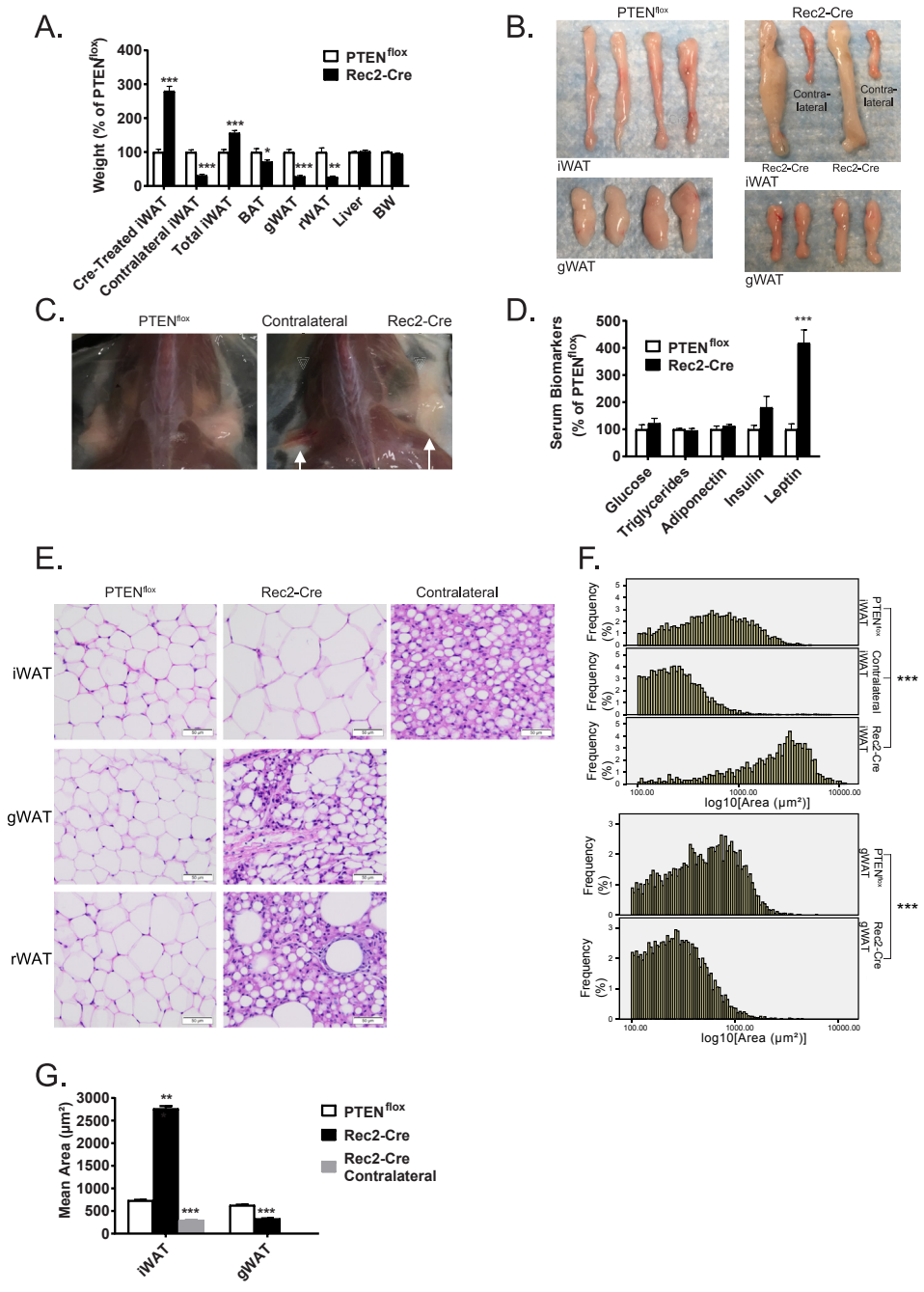


**Figure 1:** Unilateral knockdown of PTEN in the inguinal white adipose tissue redistributes whole body adiposity in male PTEN$^{flox}$ mice. (A) Normalized body and tissue weights at sacrifice, 7 weeks post AAV injection (n = 5 PTEN$^{flox}$, n = 6 Rec2-Cre). (B) Representative images of iWAT and gWAT excised at sacrifice. (C) Representative images of intact iWAT depots, dorsal view. (D) Normalized levels of serum biomarkers at sacrifice (n = 5 PTEN$^{flox}$, n = 6 Rec2-Cre). (E) Representative images of H&E stained tissue sections. (F) Quantification of cell size in the iWAT and gWAT (n = 6 per group). (G) Average size of adipocytes (n = 6 per group). Data are means ± SEM. *P < 0.05, **P < 0.01, ***P < 0.001.

collected tissues showed enlarged adipocytes in Rec2-Cre-treated iWAT whereas smaller adipocytes in the contralateral iWAT of the same mouse as well as visceral fat depots compared to PTEN$^{flox}$ controls (Figure 1E). Image analysis confirmed the hypertrophy of Cre-treated iWAT and significantly reduced size of adipocytes in the contralateral Rec2-Empty treated iWAT (Figure 1F,G). Animals receiving Rec2-Cre treatment displayed significantly reduced adipocyte size in the gWAT (Figure 1F,G).

We profiled levels of biomarkers in serum collected at sacrifice and found no significant differences in the concentrations of glucose, insulin, adiponectin, or triglycerides (Figure 1D). There was however a striking rise (approximately 4-fold) in serum leptin level in Rec2-Cre treated animals (Figure 1D).

Western blots of iWAT lysates were performed to verify knockdown of PTEN, evaluate the impact on distal insulin signaling, and detect WAT browning (Figure 2A,B). In the Rec2-Cre injected iWAT, PTEN was

 

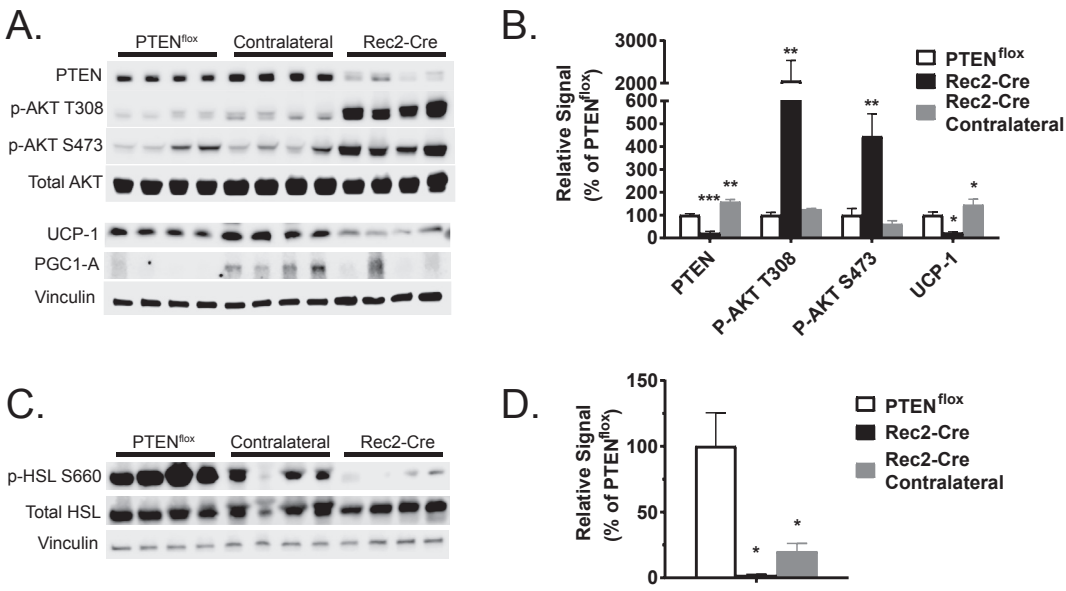


**Figure 2:** Unilateral knockdown of PTEN in the inguinal adipose tissue alters intracellular signaling in male PTEN$^{flox}$ mice. (A) Western blot of AKT and beige markers iWAT. (B) Protein quantification of western blot in (A). (C) Western blot of PKA and HSL in iWAT. (D) Protein quantification of p-HSL in (C). Data are means ± SEM, n = 4 per group. *P < 0.05, **P < 0.01.

drastically reduced and phosphorylation of AKT at S473 and T308 was significantly enhanced compared to PTEN$^{flox}$ controls. In the contralateral Rec2-Empty treated iWAT of the same mouse, protein levels of PTEN were significantly increased (Figure 2A,B). Additionally, beige cell markers including uncoupling protein 1 (UCP-1) and peroxisome proliferator-activated receptor gamma coactivator 1-alpha (PGC1-A, encoded by Ppargc1a), were significantly increased (Figure 2A,B). To examine the impact of PTEN knockdown on lipolysis, phosphorylation of HSL was determined by western blotting. Adipose knockdown of PTEN diminished phosphorylation of HSL (Figure 2C,D).

A similar experiment was performed in female PTEN$^{flox}$ mice. The results were largely consistent to findings in male mice. An approximately 3-fold increase of the Cre-treated iWAT size, a substantial decrease in visceral fat depots size, and a drastic increase of leptin level in the circulation were observed (Figure 3A–C). Gene expression was examined in the iWAT by quantitative RT-PCR. Compared to PTEN$^{flox}$ controls, the Cre-treated iWAT showed significant down-regulation of *Pten, Adrb3,* and *Hsl* whereas robust upregulation of *Lep* was observed (Figure 3D). In contrast, the contralateral iWAT of the same animal showed significant upregulation of *Pten, Ppargc1a, Ppara* (encoding peroxisome proliferator-activated nuclear receptor alpha), and *Ucp1* (Figure 3D). Moreover, Rec2-Cre injection to a single iWAT depot significantly upregulated the expression of *Pten, Ppargc1a,* and *Ucp1* in the gWAT of female mice (Figure 3E). We then profiled the hypothalamic gene expression of receptors involved in energy balance regulation. Rec2-Cre treatment had no effects on the expression of insulin receptor (*Insr*) or melanocortin receptor 4 (*Mc4r*) but resulted in upregulation of long-form leptin receptor (*Obrb*) expression (Figure 3F).

### 3.2. Knockdown of PTEN in visceral adipose

To characterize the effects of reduced PTEN expression in the visceral adipose tissue, female PTEN$^{flox}$ mice were randomized to receive a single intraperitoneal (IP) injection of $2.0 \times 10^{10}$ vg of Rec2-Cre or Rec2-Empty as a control. Our previous study revealed that the dual-cassette rAAV-Rec2 vector targets adipose tissue via IP delivery and achieves highly selective transduction of visceral fats, while significantly restricting off-target transduction of liver and resulting in no detectable transduction in others tissues, such as kidney, intestine, and testes [22].

Weekly monitoring revealed no significant decrease in food intake (Figure 4B). A significantly lower body weight was observed in Rec2-Cre injected animals by 5 weeks after Cre treatment (Figure 4A). Weekly blood draws were performed to monitor serum leptin levels and a progressive rise of serum leptin levels was observed in Rec2-Cre treated mice (Figure 4C). Rec2-Cre treatment did not affect glucose tolerance 4 weeks following rAAV injection (Figure 4D). Animals were sacrificed for collection of blood and tissue 7 weeks after rAAV injection. IP delivery of Rec2-Cre led to an approximately 4-fold increase of the mesenteric WAT (mWAT) and an approximately 2-fold increase of the gWAT, while the rWAT, iWAT and BAT were reduced (Figure 4G–I). Shrinking and beiging of the iWAT was visually apparent (Figure 4H). At sacrifice, serum leptin was robustly elevated while adiponectin level was not significantly changed when compared to mice receiving Rec2-Empty (Figure 4E,F).

### 3.3. Inhibition of AKT signaling prevents adipose PTEN knockdown-associated effects

In the adipose tissue subjected to experimental PTEN knockdown, we observed adipose hypertrophy, an increase in leptin level, and an increase in p-AKT (Figure 1 and Figure 2). As such, we asked whether AKT signaling mediates the PTEN knockdown-associated changes and thus chose MK-2206, a pan AKT inhibitor, to test this hypothesis. In pilot studies, we determined that IP injection of 50 mg/kg was a safe and efficacious dose to inhibit AKT for *in vivo* applications (Supplementary Figure 1).

PTEN$^{flox}$ mice were randomized to receive an IP injection of Rec2-Cre or AAV buffer. AKT inhibitor MK-2206 treatment was initiated two weeks after rAAV injection (Figure 5A). In the control mice without PTEN knockdown, AKT inhibitor treatment did not significantly alter iWAT mass, gWAT mass, or serum leptin levels (Figure 5B–D).

 

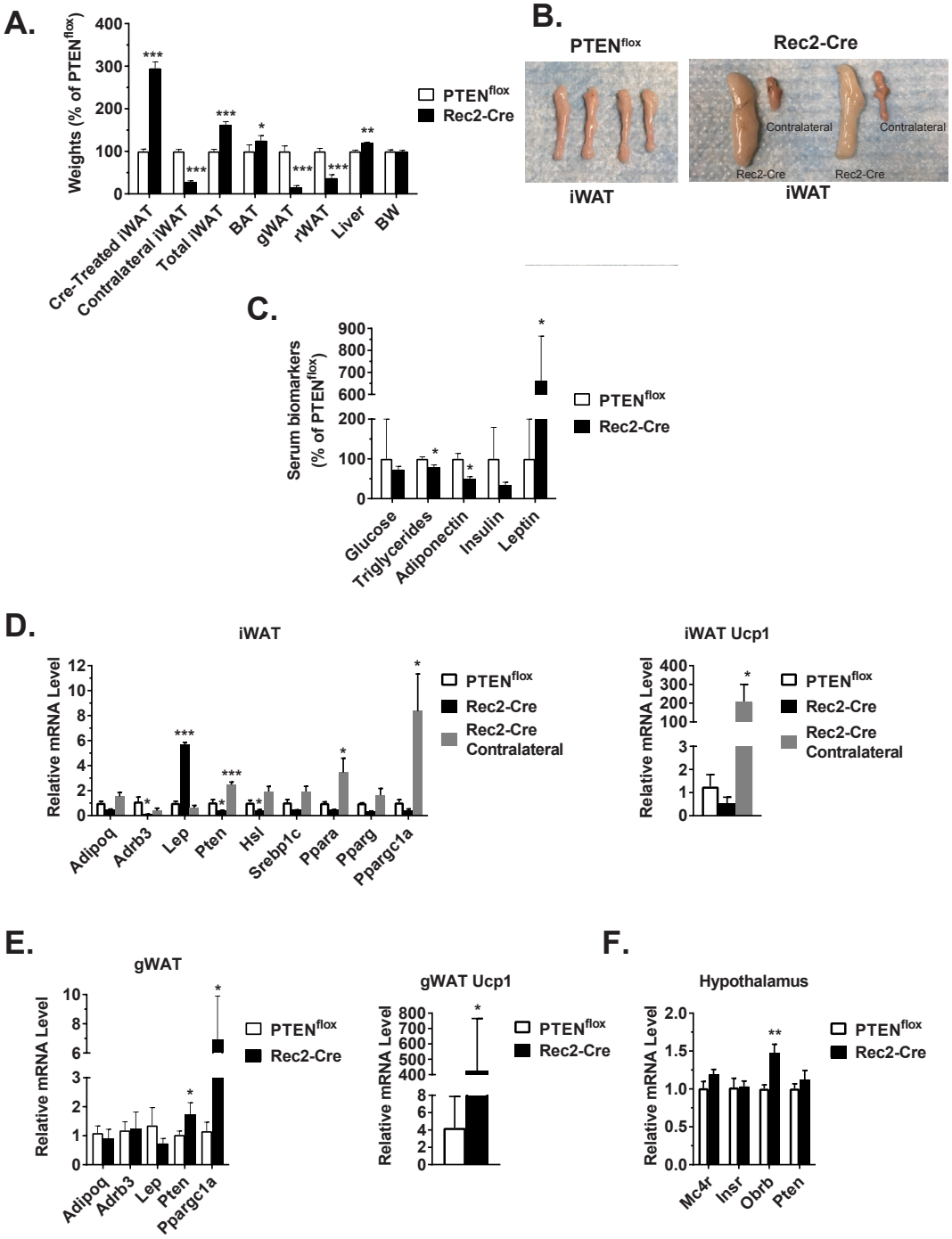


**Figure 3:** Unilateral knockdown of PTEN in the inguinal adipose tissue redistributes whole body adiposity and alters adipokine secretion and gene expression in female PTEN$^{flox}$ mice. (A) Normalized body and tissue weights at sacrifice. (B) Representative images of excised iWAT. (C) Normalized levels of serum biomarkers at sacrifice, 7 weeks after AAV injection. Data are means ± SEM (n = 4 controls, n = 5 Rec2-Cre). (D) Gene expression profile of the iWAT. (E) Gene expression profile of the gWAT. (F) Gene expression profile of the hypothalamus. Data are means ± SEM, n = 4 per group. *P < 0.05, **P < 0.01, ***P < 0.001.

Adipose PTEN protein levels were not significantly affected by AKT inhibitor treatment alone (Figure 5 E, F). Additionally, MK-2206 administration led to a slight decrease in p-AKT within control mice. Consistent with previous data, PTEN knockdown in visceral fat resulted in an approximately two-fold increase in gWAT mass, an approximately three-fold increase in serum leptin level, and an approximately four-fold increase in p-AKT in the gWAT (Figure 5C–G), all of which were blocked upon AKT inhibitor treatment (Figure 5C–G).

### 3.4. Sympathetic denervation of iWAT blocks visceral fat PTEN knockdown-induced iWAT remodeling

Regarding the PTEN knockdown-induced adipose remodeling and redistribution, we hypothesized that PTEN knockdown in one fat depot led to drastic increase of leptin level and thereby elevated sympathetic tone to other fat depots to counteract the expansion of the fat depot where PTEN was knocked down. To determine whether sympathetic innervation was required for the remodeling of untreated adipose

 

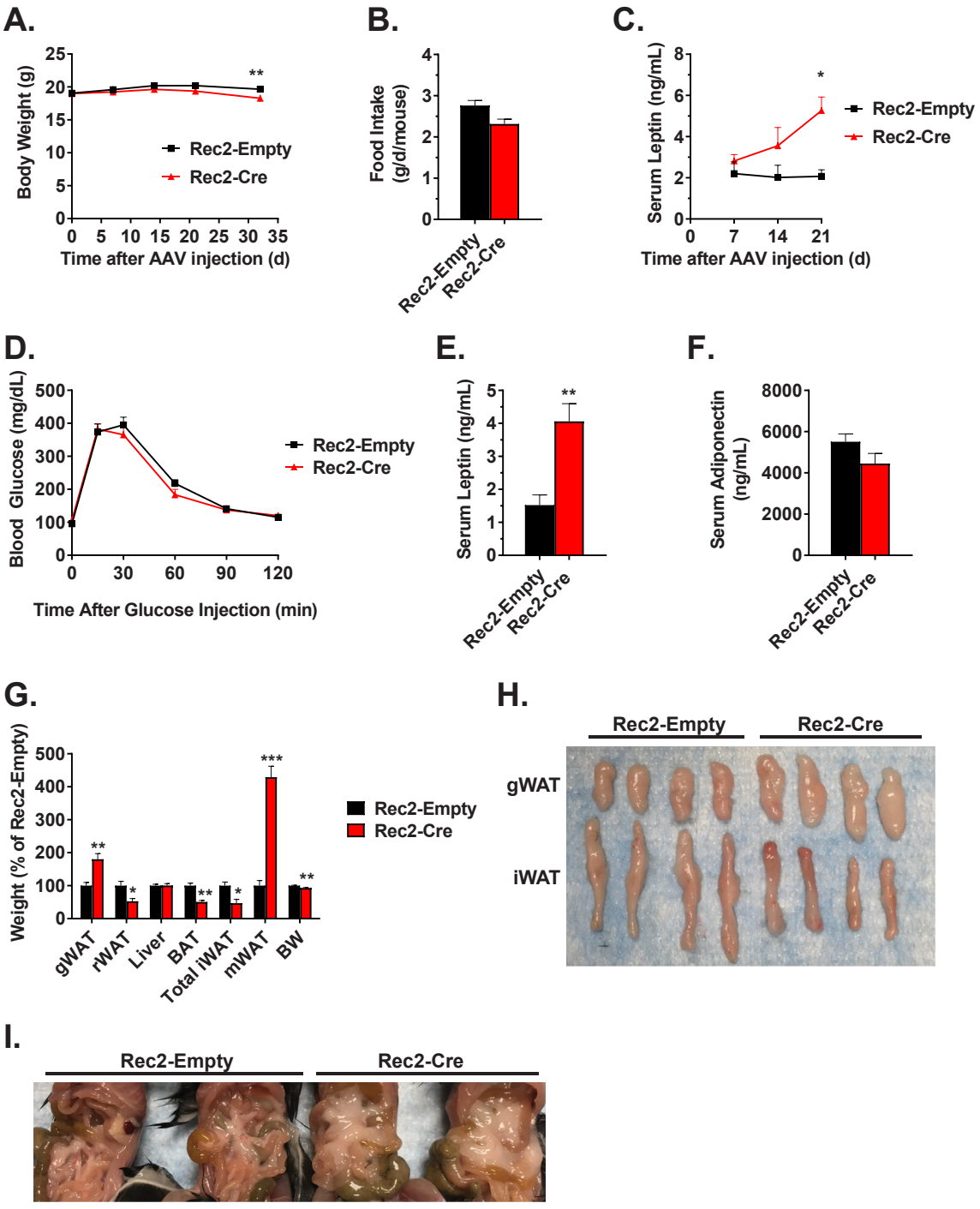


**Figure 4:** Intraperitoneal injections of Rec2-Cre redistribute whole body adiposity and alter adipokine signaling in female PTEN$^{flox}$ mice. (A) Body weight. (B) Daily food intake. Data are means ± SD. (C) Serum leptin concentrations. (D) Glucose tolerance testing 4 weeks after AAV injection. (E) Serum leptin concentrations at sacrifice. (F) Serum adiponectin concentrations at sacrifice. (G) Normalized body and tissue weights at sacrifice, 5 weeks post AAV injection. (H) Representative images of excised iWAT and gWAT depots. (I) Representative images of intact mesenteric adipose tissue. For all except (B), Data are means ± SEM (n = 5 per group) except (B). *P < 0.05, **P < 0.01, ***P < 0.001.

tissue, we performed a chemical denervation study following Rec2-Cre injections in PTEN$^{flox}$ mice, outlined in (Figure 6A). Male PTEN$^{flox}$ mice were randomly assigned to receive a single IP injection of $2.0 \times 10^{10}$ vg of Rec2-Cre or Rec2-Empty. Three days after rAAV administration, a single side of the iWAT was chemically denervated using 6-hydroxydopamine (6OHDA) [38]. Weekly monitoring revealed no significant differences in food intake or weight gain (data not shown). Mice were sacrificed 7 weeks after rAAV treatment. Rec2-Cre-treated mice showed significantly higher serum leptin level (Figure 6F), substantial enlargement of the mWAT and gWAT, and a reduction of BAT mass (Figure 6B,D), consistent with results found in female mice with IP Rec2-Cre administration (Figure 4). IP Rec2-Cre treatment caused

 

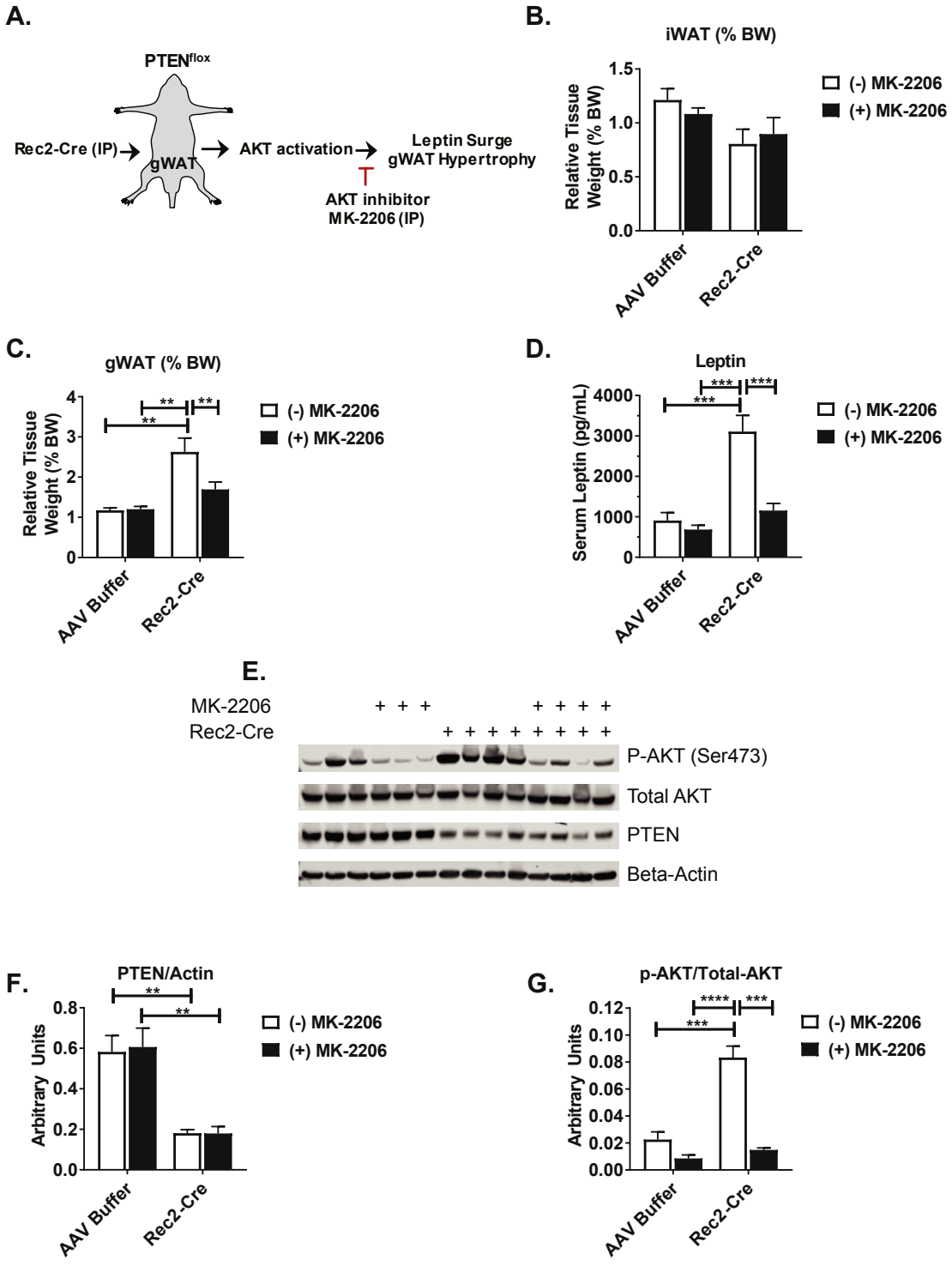


**Figure 5:** AKT inhibitor MK-2206 blocks the effects of PTEN knockdown. (A) Experimental design. (B) normalized iWAT weight. (C) normalized gWAT weight. (D) Serum leptin concentration at sacrifice. (E) Western blot of AKT and PTEN in iWAT. (F) Protein quantification of PTEN in (E). (G) Protein quantification of p-AKT in (E). Data are means ± SEM. n = 3–5 per group. *P < 0.05, **P < 0.01, ***P < 0.001.

 

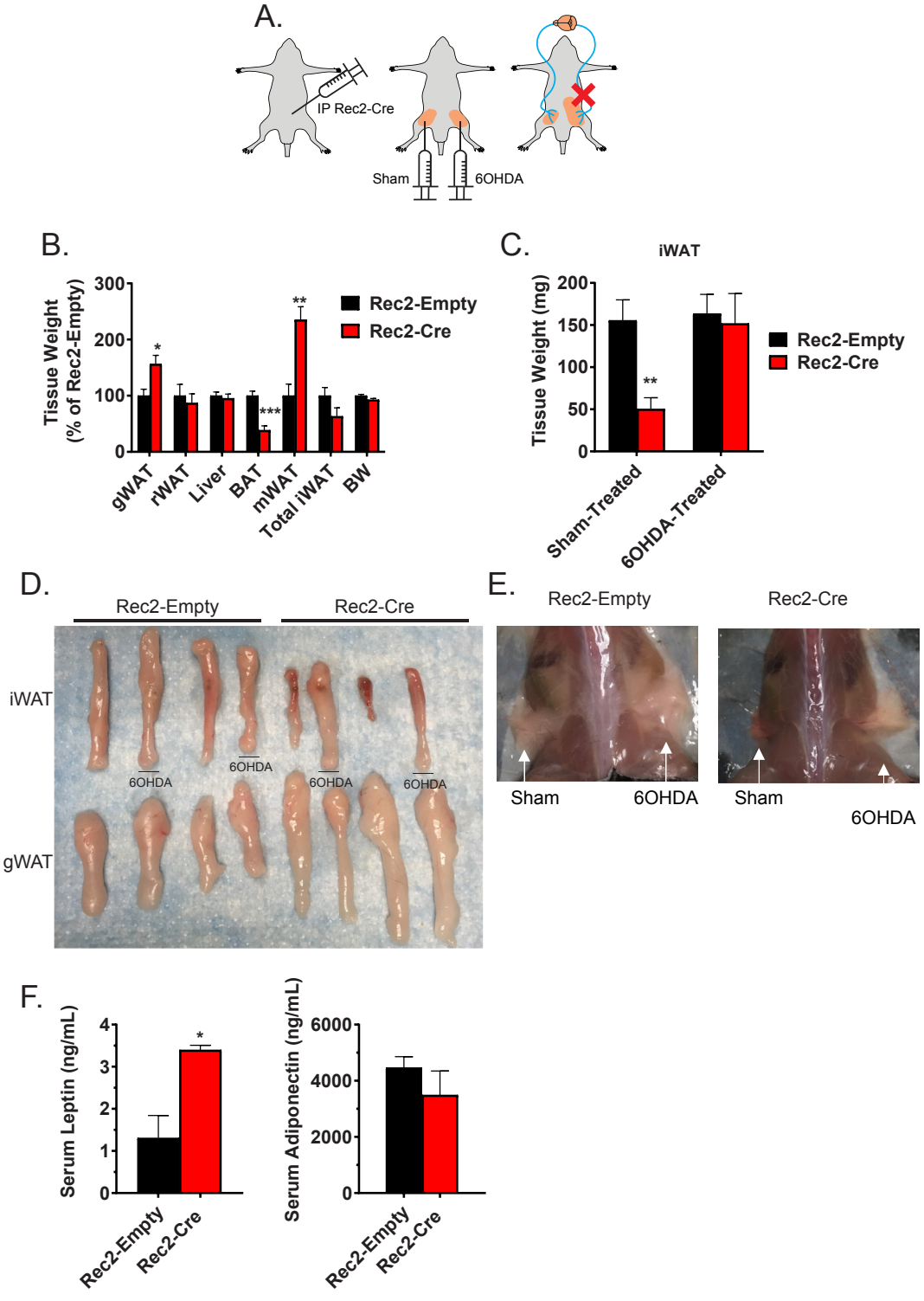


**Figure 6:** Unilateral denervation of the inguinal adipose tissue attenuates browning and reduction of fat mass in response to intraperitoneal delivery of Rec2-Cre in male PTEN$^{flox}$ mice. (A) Experimental design. (B) Normalized body and tissue weights at sacrifice. (C) Weights of sham injected and 6OHDA-denervated iWAT deposits at sacrifice. (D) Representative images of excised iWAT and gWAT. (E) Representative images of intact iWAT, dorsal view. (F) Serum leptin and adiponectin concentrations at sacrifice. Data are means ± SEM (n = 5 controls, n = 4 Rec2-Cre) except (C). *P < 0.05, **P < 0.01, ***P < 0.001.

 

involution and browning of the iWAT depot subjected to sham surgery (Figure 6C–E). In contrast, 6OHDA treatment blocked these phenotypic changes (Figure 6C–E).

### 3.5. Knockdown of hypothalamic leptin receptor attenuates the adipose redistribution induced by unilateral iWAT PTEN deficiency

Leptin exerts metabolic influence over adipose tissues through interaction with its receptors in the hypothalamus [39–41]. To examine the role of leptin in the adipose redistribution induced by PTEN knockdown in a single fat depot, we generated a microRNA targeting leptin receptor (miR-Lepr) to suppress leptin signaling (Supplementary Figure 1). A rAAV1 vector carrying the miR-Lepr was injected to the hypothalamus of PTEN$^{flox}$ mice bilaterally. A microRNA targeting no known genes was used as a control. Two weeks post hypothalamic AAV1 injection, mice of each group were randomized to receive unilateral iWAT injection of Rec2-Cre or Rec2-empty (Figure 7A). We then examined the impact of PTEN knockdown in one iWAT depot and the untreated, contralateral iWAT depot. The Lepr miRNA study design is outlined in (Figure 7A).

Hypothalamic Lepr expression in the mice receiving rAAV1-miR-Lepr was approximately 50% lower as compared to the mice receiving rAAV1-miR-scr, confirming the efficacy of miR-Lepr (Figure 7B). Changes in body weight remained similar among all four groups during the eight weeks experiment (data not shown). In mice receiving AAV1-miR-scr, iWAT injection of Rec2-Cre resulted in robust enlargement of the affected fat pad and the reduction of the contralateral untreated iWAT (Figure 7C), consistent with previous data regarding unilateral PTEN knockdown in iWAT (Figure 1). In mice receiving AAV1-miR-Lepr,

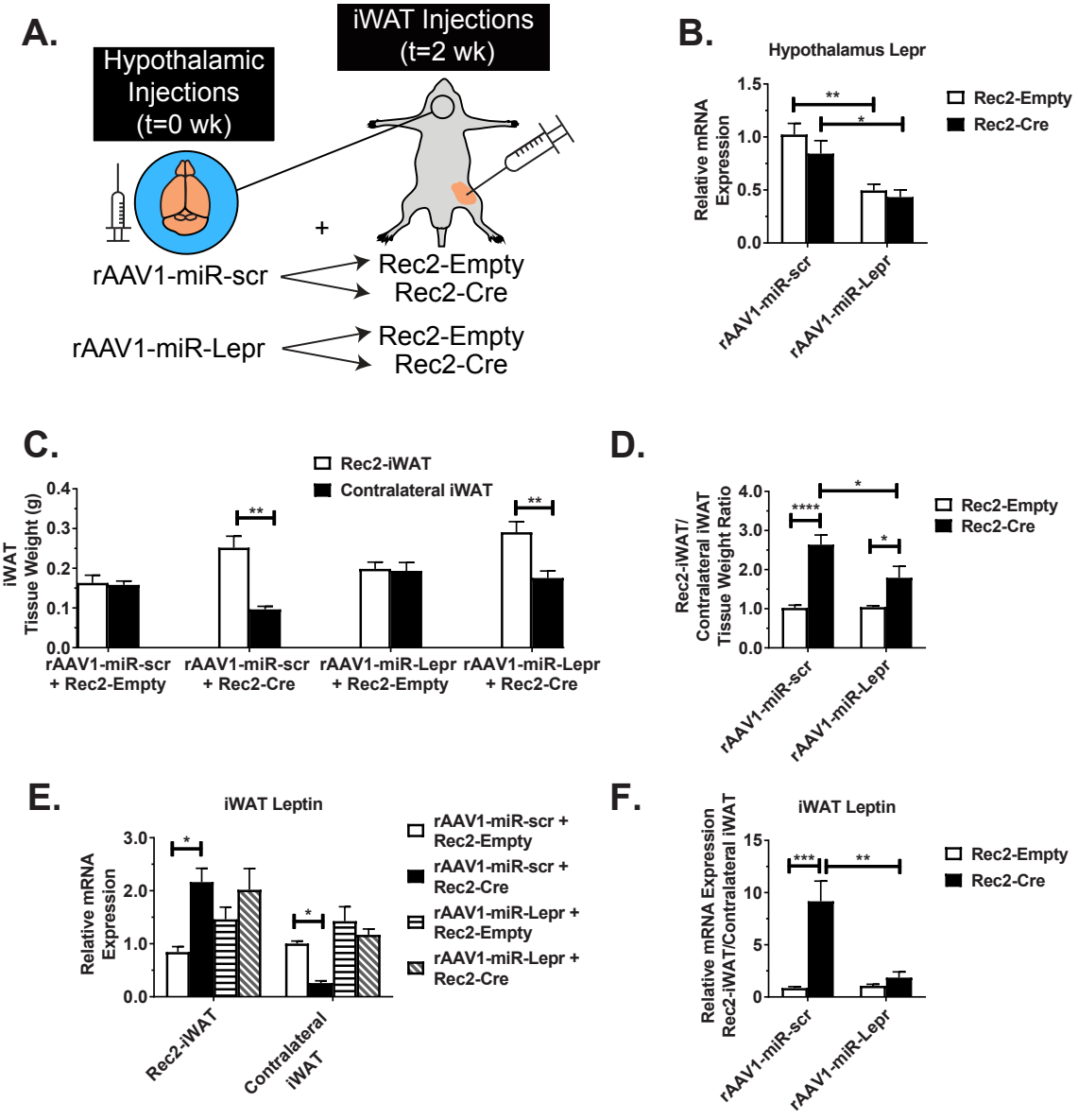


**Figure 7:** Hypothalamic leptin receptor knockdown attenuates the adipose redistribution-associated with unilateral iWAT injection of Rec2-Cre in male PTEN$^{flox}$ mice. (A) Experimental design. (B) Hypothalamic Lepr expression. (C) iWAT weight at sacrifice. (D) Ratio of Rec2-treated iWAT to the untreated contralateral iWAT. (E) Relative mRNA expression of leptin in iWAT. (F) Ratio of leptin mRNA between Rec2-treated iWAT and untreated contralateral iWAT. Data are means ± SEM. n = 6–7 per group for body weight and tissue weight data. n = 4–6 for qPCR data. *P < 0.05, **P < 0.01, ***P < 0.001.

 

Rec2-Cre-injected iWAT displayed a similar enlargement while the shrinkage of the untreated contralateral iWAT was substantially attenuated (Figure 7C). Moreover, we calculated the ratio of the Rec2-iWAT treated and the untreated contralateral iWAT of each mouse as a parameter of the selective PTEN knockdown-induced adipose redistribution. AAV1-miR-Lepr treatment significantly attenuated the iWAT redistribution (Figure 7D).

Leptin expression in iWAT tissues was analyzed by qRT-PCR (Figure 7E). In mice receiving AAV1-miR-scr, Rec2-Cre led to upregulation of *Lep* expression in the treated iWAT and downregulation of expression in the untreated contralateral iWAT, leading to drastic alteration of the ratio between the two iWAT depots (Figure 7E,F). These changes of leptin expression were completely blocked in mice receiving AAV1-miR-Lepr (Figure 7E,F). It is worthy to note that knockdown leptin receptor expression in hypothalamus by AAV-miR-Lepr slightly induced leptin expression in Rec2-iWAT (Figure 7E), a possible feedback response to central leptin receptor suppression.

## 4. DISCUSSION

Here, we found that PTEN knockdown in an individual fat pad resulted in drastic hypertrophy and mass enlargement of the affected fat depot and, in response, substantial shrinking of other fat depots, thereby leading to adipose redistribution in adult mice. Our mechanistic studies elucidate one underlying mechanism, an adipose PTEN-Leptin-Sympathetic nerve activation loop (Figure 8).

Leptin is produced and secreted predominantly from adipose tissues, and blood leptin level in the fed state correlates with adipose tissue mass [42]. Leptin levels typically mirror the extent of whole-body adiposity but can fluctuate based on feeding state [43]. Leptin secretion is enhanced in adipocytes due to insulin stimulation and this effect requires activation of the AKT pathway. In addition, AKT signaling is one of major pathway participating in adipogenesis and adipocyte proliferation [44]. In this study, AKT inhibitor treatment prevented the phenotypes of PTEN knockdown in individual fat depot including the enlargement of the PTEN-deficient adipose depot, the leptin surge, and the reduction of the contralateral depot mass. Therefore, activation of AKT signaling is downstream of PTEN knockdown and a mechanistic driver for the observed adipose redistribution feedback loop.

Leptin binds its receptors in hypothalamus to elevate central sympathetic outflow [45] and also modulates adipose lipolysis on stimulation of local nerve endings within adipose tissue [4]. Increasing plasma leptin level above the endogenous concentration by subcutaneous leptin infusion results in a dose-dependent loss of body fat content. Other studies, such as measurement of norepinephrine turnover by leptin administration and the effect of peripheral administration of leptin on 6OHDA denervation of adipose pads, suggest that leptin may act directly on adipose tissue for remodeling [46,47]. Together, previous work suggests that leptin can act both centrally—on the hypothalamus—and locally—on adipose tissue—to promote lipolysis and hypotrophy. In this study, leptin likely serves as the mediator of adipocyte PTEN deficiency-induced fat redistribution.

Our 6OHDA denervation study demonstrated that sympathetic nerve inputs blockage blunted contralateral fat mass change, indicating sympathetic outflow was required for PTEN deficiency-induced fat redistribution. Furthermore, the rAAV1-miR-Lepr mediated suppression of hypothalamic leptin receptor attenuated contralateral adipose depot mass reduction indicating the role of central leptin signaling. Together, these experiments (Figures 6 and 7) support the notion that leptin mediates the observed adipose PTEN feedback loop, at least in

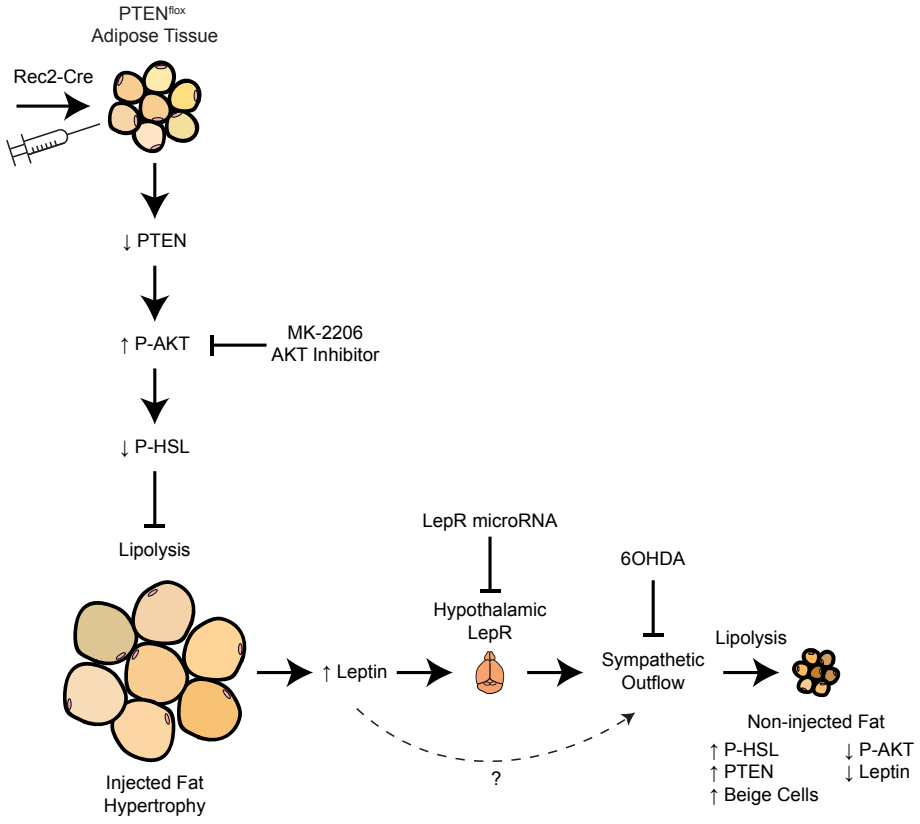


**Figure 8:** Mechanism of PTEN knockdown-induced adipose redistribution. See the Discussion for details.

 

part, through hypothalamic leptin signaling and sympathetic innervation (Figure 8). However, our study cannot rule out leptin's local direct effect on adipose remodeling also requiring intact SNS.

Of note, knockdown of PTEN in one individual fat depot resulted in compensatory upregulation of PTEN in other fat depots, suggesting a homeostatic set point of adipose PTEN. Our study reveals a regulatory loop: PTEN deficiency in one adipose depot activates the AKT pathway, inhibits lipolysis, causes adipocyte hypertrophy, and increases leptin production and release. The subsequent surge of leptin level in circulation, in part through hypothalamic leptin receptor, leads to elevation of sympathetic tone to other fat depots and thereby upregulates PTEN expression, induces beige program, and shrinks the fat mass. The "adipose PTEN-leptin—SNS—PTEN" loop contributes to the maintenance of whole-body adiposity and adipose distribution in adult animals (Figure 8).

One limitation of the study is the lack of measurement of energy expenditure. As total adipose tissue weight was not altered due to PTEN-leptin redistribution of fat, whole body energy expenditure is unlikely to be disturbed on chow diet feeding. Our results suggest that there is a homeostatic set point of adipose PTEN that is maintained via central-peripheral leptin signaling. The implied PTEN/leptin-driven energy expenditure would be in line with recent studies, which suggest that leptin is not thermogenic [48,49]. Thus, the non-thermogenic nature of leptin in whole-body metabolism merits further study.

Our results also demonstrate that local manipulation of PTEN in selective adipose depots can have a profound impact on whole body fat redistribution. However, body weight, food intake, and systemic glycemic control remained largely unaltered, which could be due to activation of insulin signaling downstream effector-AKT signaling pathway in hypertrophic adipose depots and thereby may help improve the functionality of the hypertrophic adipose depots [15]. These observations also may be due to the relative short time course of our studies using AAV-mediated manipulation compared to transgenic mouse models, lack of metabolic challenges [14,15], the regulatory loops that limit PTEN activity, or the relatively small metabolic contribution attributed to a small WAT portion. Future studies will further assess the role of adipose PTEN in long-term regulation of adiposity and systemic metabolic regulation under normal or obesogenic conditions.

In summary, our studies uncover a previously unexamined role of PTEN as a potent regulator of adipose tissue homeostasis and adipokine secretion. Furthermore, our data reveal a novel "adipose PTEN-leptin-SNS" feedback loop. A PTEN deficiency in individual adipose depot promotes hypertrophic expansion of affected adipose tissue and induces leptin surge in the circulation, which in turn activates sympathetic tone to other adipose depots to increase PTEN level, promote lipolysis, and reduce fat mass to maintain a set point of whole-body adiposity.

## AUTHOR CONTRIBUTIONS

W.H., N.J.Q., and T.B.M designed the studies, carried out the research, interpreted the results, and wrote the manuscript. S.A. carried out the research and interpreted the results. L.C. conceived the concept, designed the studies, interpreted the results, wrote, and revised the manuscript.

## ACKNOWLEDGEMENTS

We thank Jason J. Siu for technical assistance. This work was supported by NIH grants AG041250, CA166590, CA178227, CA163640 to L. Cao.

## CONFLICT OF INTEREST

All authors have no conflict of interest to declare.

## APPENDIX A. SUPPLEMENTARY DATA

Supplementary data to this article can be found online at https://doi.org/10.1016/j.molmet.2019.09.008.

## REFERENCES

[1] Bartness, T.J., Song, C.K., 2007. Thematic review series: adipocyte biology. Sympathetic and sensory innervation of white adipose tissue. The Journal of Lipid Research 48(8):1655—1672.

[2] Rosen, E.D., Spiegelman, B.M., 2014. What we talk about when we talk about fat. Cell 156(1—2):20—44.

[3] Bartness, T.J., Liu, Y., Shrestha, Y.B., Ryu, V., 2014. Neural innervation of white adipose tissue and the control of lipolysis. Frontiers in Neuroendocrinology 35(4):473—493.

[4] Zeng, W., Pirzgalska, R.M., Pereira, M.M., Kubasova, N., Barateiro, A., Seixas, E., et al., 2015. Sympathetic neuro-adipose connections mediate leptin-driven lipolysis. Cell 163(1):84—94.

[5] Jiang, H., Ding, X., Cao, Y., Wang, H., Zeng, W., 2017. Dense intra-adipose sympathetic arborizations are essential for cold-induced beiging of mouse white adipose tissue. Cell Metabolism 26(4), 686—692.e3.

[6] Cao, L., Choi, E.Y., Liu, X., Martin, A., Wang, C., Xu, X., et al., 2011. White to brown fat phenotypic switch induced by genetic and environmental activation of a hypothalamic-adipocyte axis. Cell Metabolism 14(3):324—338.

[7] Bachman, E.S., Dhillon, H., Zhang, C.Y., Cinti, S., Bianco, A.C., Kobilka, B.K., et al., 2002. betaAR signaling required for diet-induced thermogenesis and obesity resistance. Science 297(5582):843—845.

[8] Brasaemle, D.L., 2007. Thematic review series: adipocyte biology. The perilipin family of structural lipid droplet proteins: stabilization of lipid droplets and control of lipolysis. The Journal of Lipid Research 48(12):2547—2559.

[9] Nakanishi, A., Kitagishi, Y., Ogura, Y., Matsuda, S., 2014. The tumor suppressor PTEN interacts with p53 in hereditary cancer (Review). International Journal of Oncology 44(6):1813—1819.

[10] Li, J., Yen, C., Liaw, D., Podsypanina, K., Bose, S., Wang, S.I., et al., 1997. PTEN, a putative protein tyrosine phosphatase gene mutated in human brain, breast, and prostate cancer. Science 275(5308):1943—1947.

[11] Stambolic, V., Suzuki, A., de la Pompa, J.L., Brothers, G.M., Mirtsos, C., Sasaki, T., et al., 1998. Negative regulation of PKB/Akt-dependent cell survival by the tumor suppressor PTEN. Cell 95(1):29—39.

[12] Chalhoub, N., Baker, S.J., 2009. PTEN and the PI3-kinase pathway in cancer. Annual Review of Pathology 4:127—150.

[13] Ortega-Molina, A., Serrano, M., 2013. PTEN in cancer, metabolism, and aging. Trends in Endocrinology and Metabolism 24(4):184—189.

[14] Kurlawalla-Martinez, C., Stiles, B., Wang, Y., Devaskar, S.U., Kahn, B.B., Wu, H., 2005. Insulin hypersensitivity and resistance to streptozotocin-induced diabetes in mice lacking PTEN in adipose tissue. Molecular and Cellular Biology 25(6):2498—2510.

[15] Morley, T.S., Xia, J.Y., Scherer, P.E., 2015. Selective enhancement of insulin sensitivity in the mature adipocyte is sufficient for systemic metabolic improvements. Nature Communications 6:7906.

[16] Sanchez-Gurmaches, J., Hung, C.M., Sparks, C.A., Tang, Y., Li, H., Guertin, D.A., 2012. PTEN loss in the Myf5 lineage redistributes body fat and reveals subsets of white adipocytes that arise from Myf5 precursors. Cell Metabolism 16(3):348—362.

 

[17] Ortega-Molina, A., Efeyan, A., Lopez-Guadamillas, E., Munoz-Martin, M., Gomez-Lopez, G., Canamero, M., et al., 2012. Pten positively regulates brown adipose function, energy expenditure, and longevity. Cell Metabolism 15(3):382—394.

[18] Garcia-Cao, I., Song, M.S., Hobbs, R.M., Laurent, G., Giorgi, C., de Boer, V.C., et al., 2012. Systemic elevation of PTEN induces a tumor-suppressive metabolic state. Cell 149(1):49—62.

[19] Ro, H.S., Zhang, L., Majdalawieh, A., Kim, S.W., Wu, X., Lyons, P.J., et al., 2007. Adipocyte enhancer-binding protein 1 modulates adiposity and energy homeostasis. Obesity (Silver Spring) 15(2):288—302.

[20] Gorbenko, O., Panayotou, G., Zhyvoloup, A., Volkova, D., Gout, I., Filonenko, V., 2010. Identification of novel PTEN-binding partners: PTEN interaction with fatty acid binding protein FABP4. Molecular and Cellular Biochemistry 337(1—2): 299—305.

[21] Liu, X., Magee, D., Wang, C., McMurphy, T., Slater, A., During, M., et al., 2014. Adipose tissue insulin receptor knockdown via a new primate-derived hybrid recombinant AAV serotype. Molecular Therapy Methods & Clinical Development 1:8.

[22] Huang, W., Liu, X., Queen, N.J., Cao, L., 2017. Targeting visceral fat by intraperitoneal delivery of novel AAV serotype vector restricting off-target transduction in liver. Molecular Therapy-Methods & Clinical Development 6:68—78.

[23] Huang, W., McMurphy, T., Liu, X., Wang, C., Cao, L., 2016. Genetic manipulation of Brown fat via oral administration of an engineered recombinant adeno-associated viral serotype vector. Molecular Therapy 24(6):1062—1069.

[24] Zhu, Y., Gao, Y., Tao, C., Shao, M., Zhao, S., Huang, W., et al., 2016. Connexin 43 mediates white adipose tissue beiging by facilitating the propagation of sympathetic neuronal signals. Cell Metabolism 24(3):420—433.

[25] Ng, R., Hussain, N.A., Zhang, Q., Chang, C., Li, H., Fu, Y., et al., 2017. miRNA-32 drives Brown fat thermogenesis and trans-activates subcutaneous white fat browning in mice. Cell Reports 19(6):1229—1246.

[26] Zhang, Y., Xie, L., Gunasekar, S.K., Tong, D., Mishra, A., Gibson, W.J., et al., 2017. SWELL1 is a regulator of adipocyte size, insulin signalling and glucose homeostasis. Nature Cell Biology 19(5):504—517.

[27] Xiao, R., Bergin, S.M., Huang, W., Mansour, A.G., Liu, X., Judd, R.T., et al., 2019. Enriched environment regulates thymocyte development and alleviates experimental autoimmune encephalomyelitis in mice. Brain, Behavior, and Immunity 75:137—148.

[28] Charbel Issa, P., De Silva, S.R., Lipinski, D.M., Singh, M.S., Mouravlev, A., You, Q., et al., 2013. Assessment of tropism and effectiveness of new primate-derived hybrid recombinant AAV serotypes in the mouse and primate retina. PLoS One 8(4):e60361.

[29] Huang, W., Queen, N.J., Cao, L., 2019. rAAV-mediated gene delivery to adipose tissue. Methods in Molecular Biology (Clifton, NJ) 1950:389—405.

[30] Cao, L., Liu, X., Lin, E.J., Wang, C., Choi, E.Y., Riban, V., et al., 2010. Environmental and genetic activation of a brain-adipocyte BDNF/leptin axis causes cancer remission and inhibition. Cell 142(1):52—64.

[31] Cao, L., Lin, E.J., Cahill, M.C., Wang, C., Liu, X., During, M.J., 2009. Molecular therapy of obesity and diabetes by a physiological autoregulatory approach. Nature Medicine 15(4):447—454.

[32] Livak, K.J., Schmittgen, T.D., 2001. Analysis of relative gene expression data using real-time quantitative PCR and the 2(-Delta Delta C(T)) Method. Methods 25(4):402—408.

[33] Rueden, C.T., Schindelin, J., Hiner, M.C., DeZonia, B.E., Walter, A.E., Arena, E.T., et al., 2017. ImageJ2: ImageJ for the next generation of scientific image data. BMC Bioinformatics 18(1):529.

[34] Schindelin, J., Arganda-Carreras, I., Frise, E., Kaynig, V., Longair, M., Pietzsch, T., et al., 2012. Fiji: an open-source platform for biological-image analysis. Nature Methods 9(7):676—682.

[35] Galarraga, M., Campion, J., Munoz-Barrutia, A., Boque, N., Moreno, H., Martinez, J.A., et al., 2012. Adiposoft: automated software for the analysis of white adipose tissue cellularity in histological sections. The Journal of Lipid Research 53(12):2791—2796.

[36] Otsu, n, 1979. A threshold selection method from gray-level histograms. IEEE Transactions on Systems, Man, and Cybernetics 9:62—69.

[37] Legland, D., Arganda-Carreras, I., Andrey, P., 2016. MorphoLibJ: Integrated library and plugins for mathematical morphology with ImageJ. Bioinformatics 32(22):3532—3534.

[38] During, M.J., Liu, X., Huang, W., Magee, D., Slater, A., McMurphy, T., et al., 2015. Adipose VEGF links the white-to-Brown fat switch with environmental, genetic, and pharmacological stimuli in male mice. Endocrinology 156(6): 2059—2073.

[39] Lee, G.H., Proenca, R., Montez, J.M., Carroll, K.M., Darvishzadeh, J.G., Lee, J.I., et al., 1996. Abnormal splicing of the leptin receptor in diabetic mice. Nature 379(6566):632—635.

[40] Levin, N., Nelson, C., Gurney, A., Vandlen, R., de Sauvage, F., 1996. Decreased food intake does not completely account for adiposity reduction after ob protein infusion. Proceedings of the National Academy of Sciences of the U S A 93(4):1726—1730.

[41] Vaisse, C., Halaas, J.L., Horvath, C.M., Darnell Jr., J.E., Stoffel, M., Friedman, J.M., 1996. Leptin activation of Stat3 in the hypothalamus of wild-type and ob/ob mice but not db/db mice. Nature Genetics 14(1):95—97.

[42] Maffei, M., Halaas, J., Ravussin, E., Pratley, R.E., Lee, G.H., Zhang, Y., et al., 1995. Leptin levels in human and rodent: measurement of plasma leptin and ob RNA in obese and weight-reduced subjects. Nature Medicine 1(11):1155—1161.

[43] Munzberg, H., Morrison, C.D., 2015. Structure, production and signaling of leptin. Metabolism - Clinical and Experimental 64(1):13—23.

[44] Ghaben, A.L., Scherer, P.E., 2019. Adipogenesis and metabolic health. Nature Reviews Molecular Cell Biology 20(4):242—258.

[45] Satoh, N., Ogawa, Y., Katsuura, G., Numata, Y., Tsuji, T., Hayase, M., et al., 1999. Sympathetic activation of leptin via the ventromedial hypothalamus: leptin-induced increase in catecholamine secretion. Diabetes 48(9):1787—1793.

[46] Penn, D.M., Jordan, L.C., Kelso, E.W., Davenport, J.E., Harris, R.B., 2006. Effects of central or peripheral leptin administration on norepinephrine turnover in defined fat depots. American Journal of Physiology Regulatory, Integrative and Comparative Physiology 291(6):R1613—R1621.

[47] Rooks, C.R., Penn, D.M., Kelso, E., Bowers, R.R., Bartness, T.J., Harris, R.B., 2005. Sympathetic denervation does not prevent a reduction in fat pad size of rats or mice treated with peripherally administered leptin. American Journal of Physiology Regulatory, Integrative and Comparative Physiology 289(1):R92—R102.

[48] Fischer, A.W., Hoefig, C.S., Abreu-Vieira, G., de Jong, J.M.A., Petrovic, N., Mittag, J., et al., 2016. Leptin raises defended body temperature without activating thermogenesis. Cell Reports 14(7):1621—1631.

[49] Kaiyala, K.J., Ogimoto, K., Nelson, J.T., Muta, K., Morton, G.J., 2016. Physiological role for leptin in the control of thermal conductance. Molecular Metabolism 5(10):892—902.

 